

## Electric-field effects in resistive oxides: facts and artifacts

B. Fisher, J. Genossar, L. Patlagan and G. M. Reisner

Physics Department, Technion, Haifa 32000, Israel

**Abstract.** Striking non-linear conductivity effects induced by surprisingly low electric-fields in charge-ordered oxides, were reported variously as dielectric breakdown, charge-order collapse, depinning of charge-density-waves or other electronic effects. Our pulsed and d.c. I-V measurements on resistive oxides show that non-linear conductivity of electronic origin at low electric-fields is a rare phenomenon. In the majority of cases we detected no deviations from linearity in pulsed I-V characteristics under fields up to  $E \sim 500$  V/cm. Current-controlled negative-differential-resistance (NDR) and hysteresis were found in d.c. measurements at fields that decrease with increasing temperatures, a behavior typical of Joule heating in materials with negative temperature coefficient of resistivity. For the d.c. I-V characteristics of our samples exhibiting NDR, we found a rather unexpected correlation between  $\rho(E_m)$  - the resistivity at maximum field (at the onset of NDR) and  $\rho(E=0)$  - the ohmic resistivity. The data points for  $\rho(E_m)$  versus  $\rho(E=0)$  obtained from such characteristics of 13 samples (8 manganites, 4 nickelates and one multiferroic) at various ambient temperatures, plotted together on a log-log scale, follow closely a linear dependence with slope one that spans more than five orders of magnitude. This dependence is reproduced by several simple models.

### 1 Introduction

The *non-linear conductivity* of resistive materials and related effects, may be of *electronic origin* (NCEO) such as dielectric breakdown [1], Zener-type tunneling [2], field enhanced hopping [3], impact ionization [4], the Gunn effect [5], the acoustoelectric effect [6], depinning of charge-density-waves (CDW) [7], etc. It may also be a self-heating effect – *an artifact*. In order to distinguish between NCEO and self-heating effects one can use an old and simple technique based on the comparison of pulsed and d.c. I-V characteristics carried out on the same sample [8]. In this report we first compare an example of NCEO with one of pure self-heating and show how easily these two types of behavior can be recognized. Following this, our emphasis will be on the self-heating effects and their typical behavior since they are frequent and could be misleading. The results of calculations for several simple models of negative-differential conductivity (NDR) due to self-heating will be compared with experimental results. The role of the resistance connected in series with the sample (the load resistance) in triggering switching or current runaway will be discussed and shown to apply to some recent claims of an electric-field-induced phase transition.

### 2 NCEO versus self-heating

In figure 1 we compare the d.c. and I-V characteristics of an Mn-deficient (LaCa)MnO<sub>3</sub> sample [9] which exhibits

NCEO due to field-enhanced hopping, with that of a charge-ordered sample of La<sub>0.25</sub>Ca<sub>0.75</sub>MnO<sub>3</sub> [8] which does not show NCEO. The temperature dependence of the ohmic resistivity,  $\rho(T)$ , of La<sub>0.77</sub>Ca<sub>0.23</sub>Mn<sub>0.96</sub>O<sub>3</sub> (see figure 1 (a)) is activated due to the disorder-induced localization by the Mn vacancies. A typical example of d.c. and pulsed J-E characteristic for this sample at the ambient temperature of 80 K is shown in figure 1 (b). The J(E) pulsed measurements (symbols) exhibit strong non-linearity. Nevertheless, no time dependence of the voltage is observed over the duration of the applied pulses (of the order of msecs.). At fixed current, for pulses of longer durations, of the order of tens or hundreds msecs. the voltage drops become time dependent. The d.c. plot of J(E) (solid curve), that could be measured down to very low currents, is linear at low fields, but becomes strongly non-linear at high fields. The dotted line represents the ohmic current density extrapolated from the low-field d.c. characteristic. At the start of the non-linear regime the d.c. and pulsed measurements overlap, but at an unpredictable higher field the d.c. plot deviates from the pulsed one and exhibits NDR and hysteresis. This is due to self-heating that masks the electronic effect.

La<sub>0.25</sub>Ca<sub>0.75</sub>MnO<sub>3</sub> belongs to the family of La<sub>1-x</sub>Ca<sub>x</sub>MnO<sub>3</sub> ( $x > 0.5$ ) famous for charge ordering that sets in at temperatures which depend on  $x$ . The charge-ordered compounds are non-metallic and their conductivity is activated (with constant or variable activation energies). The temperature dependence of the ohmic resistivity ( $\rho$ ) of La<sub>0.25</sub>Ca<sub>0.75</sub>MnO<sub>3</sub> is shown in

figure 1(c). The charge ordering transition is observed around 200 K; at lower temperatures the resistivity is activated. The pulsed and d.c. J-E characteristics of this sample at 80 K are shown in figure 1(d). The pulsed  $J(E)$  plot is linear up to the highest applied field ( $\sim 230$  V/cm) while the d.c. measurements show NDR at a field lower by about one order of magnitude.

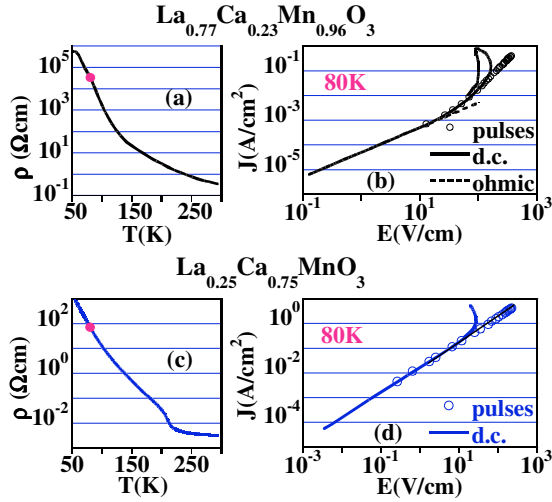


**Fig. 1** (a) Temperature dependence of resistivity of  $\text{La}_{0.77}\text{Ca}_{0.23}\text{MnO}_3$ . (b) Current density as function of electric field at 80 K, measured with d.c. (solid line) and single short pulses (symbols); dashed line- extrapolated ohmic current. (c) Temperature dependence of resistivity of the charge-ordered  $\text{La}_{0.25}\text{Ca}_{0.75}\text{MnO}_3$ . (d) Pulsed and d.c. J-E characteristic of this sample at 80 K. The red dots in (a) and (c) mark the temperature of the I-V measurements.

Presumably, the great interest in electric-field effects in charge-ordered manganites, sometimes called colossal electroresistance, was driven by the dramatic colossal magnetoresistance found in manganites in another part of their phase diagram. It was believed for a long time that high electric fields cause depinning or melting of the charge-order, leading to non-linear conductivity [8,10]. Motivated by the numerous publications on non-linear conductivity in various resistive oxides, based on d.c. measurements or on trains of pulses (which approach d.c. measurements) we carried out many I-V measurements. Our experience shows that NCEO in resistive oxides is a rare phenomenon and in particular it is absent in all the charge-ordered oxides that we investigated (manganites [8], nickelates [10], and  $\text{LuFe}_2\text{O}_4$  - a compound regarded as multiferroic [11]).

For years, we treated self-heating as a nuisance, an artifact. However, the large number of our results accumulated over the years shows that in spite of the many parameters that affect self-heating, such as temperature dependence of resistivity, geometry, heat capacity, heat conduction, thermal contact with the sample holder, one can find some systematics in the self-heating J-E characteristics.

The main observation is that for all the investigated samples in which NCEO is absent and the d.c. non-linear

conductivity is due to self-heating, the threshold field of NDR ( $E_m = E(dE/dJ=0)$ ) decreases with increasing temperature. As a representative example of our results, we show in figure 2  $J(E)$  of the  $\text{La}_{0.25}\text{Ca}_{0.75}\text{MnO}_3$  sample. The inset of this figure shows the ohmic resistivity  $\rho(E=0)$  (vertical axis at left) and the maximal field -  $E_m$  (vertical axis at right) as function of temperature; also shown is the resistivity at the onset of NDR as function of temperature ( $\rho(E_m) = E_m/J(E_m)$ ). The error bars of the three variables in the inset of figure 2, obtained from the data file for increasing current, are much smaller than the sizes of the symbols. Note that the scale at left spans twice the number of orders of magnitude of that at right. The three traces are practically parallel, indicating that roughly  $E_m^{1/2} \propto \rho(E_m) \propto \rho(E=0)$ . Interestingly, the hysteresis of the d.c. J-E characteristic in figure 1(b), where the non-linearity due to self-heating is superimposed on very large NCEO, is much larger than the barely distinguishable hysteresis in figures 1(d) and 2 where the non-linearity is due to self-heating only.

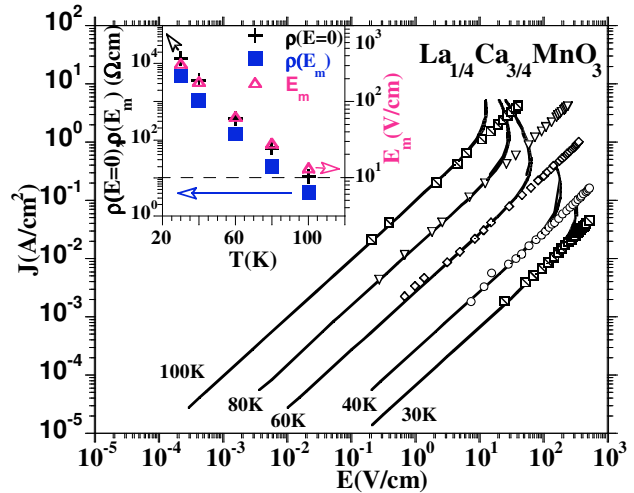


**Fig. 2.** Pulsed (symbols) and d.c. (solid lines) J-E characteristic of the  $\text{La}_{0.25}\text{Ca}_{0.75}\text{MnO}_3$  sample at various temperatures. Note the onset of NDR at  $E_m$  that decreases with increasing temperature. Inset:  $\rho(E=0)$ ,  $\rho(E_m)$  (scale at right) and  $E_m$  (scale at left) versus T.

We checked our previous results and found that proportionality between  $\rho(E_m)$  and  $\rho(E=0)$  seems to be a good approximation. The data points for  $\rho(E_m)$  versus  $\rho(E=0)$  obtained from the J-E characteristics of 13 samples (8 manganites, 4 nickelates and one compound regarded as multiferroic -  $\text{LuFe}_2\text{O}_4$ ) at various ambient temperatures, are plotted together on log-log scale in figure 3.

Surprisingly, the data points of figure 3 follow closely a linear dependence with slope one that spans more than five orders of magnitude. The fitted (dashed) line represents  $\rho(E_m) = 0.36\rho(E=0)$ , with Pearson's Correlation Coefficient  $R^2 = 0.895$ . The traces of  $E_m^{1/2}$  versus  $\rho(E=0)$  did not coalesce into one broad line as in the case of  $\rho(E_m)$  versus  $\rho(E=0)$ ; this is due to the sensitivity of  $E_m$  to the various parameters involved in self-heating.

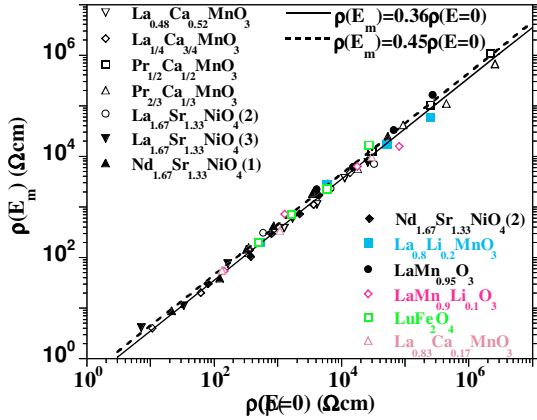


**Fig. 3.**  $\rho(E_m)$  versus  $\rho(E=0)$  obtained from the d.c. J-E characteristics for 13 different samples with activated resistivities: 8 manganites, 4 nickelates and one multiferroic ( $\text{LuFe}_2\text{O}_4$ ). The linear fit to the data is represented by the solid line; the dashed line shows the result of model 3 (see below).

### 3 Negative differential resistivity (NDR) due to Joule heating

The effect of Joule heating on the I-V characteristics of conductors has been discussed in the literature since the end of the 19-th century [12] but the topic attracted exceptional attention only much later [13], after the discovery of switching in an amorphous semiconductor. In order to mimic the remarkable behavior of the experimental  $\rho(E_m)$  versus  $\rho(E=0)$  we calculated the ratio  $\rho(E_m)/\rho(E=0)$  for three models with different geometries. For all three models we assumed, as in Refs.[13] and [14], that  $\rho(T_o+\Delta T)=\rho(T_o)\exp(-\Delta T/T_a)$  where  $T_o$  is the ambient temperature,  $\Delta T$  is the excess temperature of the sample above ambient temperature, and  $T_a$  – a constant. This is a good approximation for activated transport ( $\rho \propto \exp(-T_n/T)$  where  $n \leq 1$  and  $T_n$  a corresponding constant) when  $\Delta T \ll T_n$  (see in figure 1 (a) and (c) that in the vicinity of each  $T$  the curves are practically linear).

**Model 1.** This is the simplest model, similar to Model B of Ref. [13]. We assumed steady state conditions with uniform temperature rise  $\Delta T$  in a bar-shaped sample; then, the uniform Joule power density  $E^2/\rho$  was equated with Newton's cooling law ( $-Q=\alpha \Delta T$ ):

$$E^2 = \rho(T_o + \Delta T)\alpha\Delta T \quad \alpha T_a \rho(T_o) \ln\left(\frac{\rho(T_o)}{\rho(T_o + \Delta T)}\right) \quad (1)$$

The field at the onset of NDR is given by  $dE/d\Delta T=0$ . This yields:

$$\ln\left(\frac{\rho(T_o)}{\rho(T_o + \Delta T(E_m))}\right) = 1, \quad \frac{\rho(T_o + \Delta T(E_m))}{\rho(T_o)} = \frac{\rho(E_m)}{\rho(E=0)} = e^{-1} = 0.37 \quad (2)$$

This ratio does not depend on  $T_a$  nor on  $\alpha$  and is very close to the ratio obtained from the experimental results

(see figure 3). It is also clear from equation 1 that  $E_m$  is sample-dependent, since it is a function of  $\alpha T_a \rho(T_o)$ .

**Model 2.** The assumed geometry of the sample is that of a cylindrical bar with the envelope kept at the ambient temperature. The dependence of the excess temperature on the distance from the cylinder's axis was obtained in Ref. [14] by solving a second order differential equation of heat conduction. Here  $E$  is a constant but  $J$  is a function of the radius; the result is better expressed in terms of current ( $I$ ) and voltage ( $V$ ).  $I(V)$  obtained in this case yields  $R(V_m)/R(V=0)=0.35$ , independent of the parameters entering the problem ( $T_a$  and the heat conductivity). Here  $R(V_m)=V_m/I(V_m)$ .

**Model 3.** The geometry is that of a thin platelet with the bottom face kept at ambient temperature. The second order differential equation for heat conduction along the height of the platelet can be reduced to a differential equation of the first order that apparently does not yield a simple analytic solution. Therefore, we solved it numerically and integrated  $J$  over the cross-section. The solution yields  $R(V_m)/R(V=0)=0.45$ .

Figure 4 shows the normalized  $i-v$  curves for the three models, where  $i=I/I(V_m)$  and  $v=V/V_m$ . Up to the onset of NDR the three curves are close but they separate for  $i>1$ .

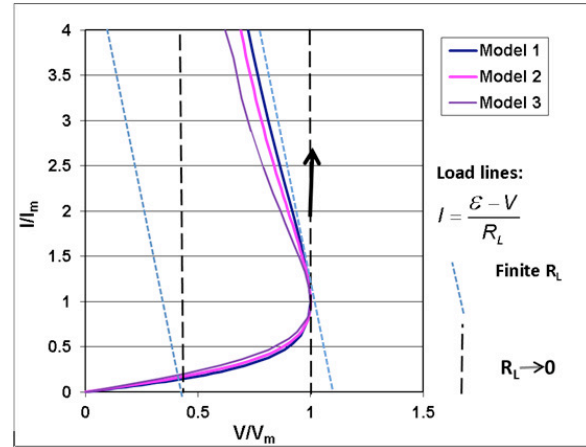


**Fig. 4.** Normalized  $i(=I/I(V_m)) - v(=V/V_m)$  characteristics for the three models described in the text. Two pairs of parallel load lines ( $I=(\mathcal{E}-V)/R_L$ ) corresponding to finite (dotted) or negligible (dashed) load resistances are superimposed on the characteristics.  $\mathcal{E}$  is the applied voltage and  $R_L$  is the load resistance.

The actual I-V characteristic as measured in the NDR regime, depends on the properties of the source whether constant current, constant voltage or intermediate. It is seen that switching from low to high current occurs when the dotted line is tangent to the characteristics. Runaway of the current occurs under constant voltage conditions ( $R_L \rightarrow 0$ ) when the vertical load line touches  $V_m$  (see arrow in figure 4).

J-E characteristics of  $\text{LuFe}_2\text{O}_4$  that exhibit current runaway, as seen in figure 4 for  $R_L \rightarrow 0$ , have been reported in several articles [15] and have been interpreted as a phase transition induced by the electric-field. With decreasing temperatures, the vertical portions of their characteristics are shifted to lower fields, thus in favor of current runaway in the regime of thermal NDR. In reference [15] the thermal runaway was limited by restricting the current to finite values (equivalent to a small load resistance). Our pulsed J-E characteristics of  $\text{LuFe}_2\text{O}_4$  are perfectly linear up to  $\sim 480$  V/cm (far higher than the maximal fields in reference [15]). We used single pulses much shorter than theirs (1 - 4 msec duration); for long (100 msec) constant current pulses the voltage drops between probes exhibit strong time dependence (see figure 3 in reference 9) caused by self-heating. Our d.c. J-E characteristics of  $\text{LuFe}_2\text{O}_4$  resemble those in Fig. 2. Simultaneous infrared and transport measurements under d.c. current confirmed that the strong electro-resistance of  $\text{LuFe}_2\text{O}_4$  is a self-heating effect [16]. The authors of an earlier report [17] have reached the same conclusion based on neutron diffraction measurements on a  $\text{LuFe}_2\text{O}_4$  sample under high electric field.

#### 4 Conclusion

We have shown here that the old technique of I-V characteristics obtained using a pulse generator and a memory scope is very efficient in avoiding self-heating artifacts. It is much faster and much cheaper than the elaborate experiments described in Refs. [16] and [17], in discriminating between simple facts and dramatic artifacts. In spite of the fact that self-heating seems to be a messy process we did find a surprisingly simple dependence between the resistivity at the onset of NDR and the resistivity at ambient temperature, a relation that holds for many samples.

#### References

1. J.J. O'Dwyer, *Advances in Physics* **7**, 349 (1958)
2. C. Zener, *Proc. R. Soc. Lond. A* **145**, 523 (1934)
3. H. Böttger and V.V. Bryksin, *Hopping Conduction in Solids*, VCH Akademie-Verlag, Berlin, 1985
4. S.M. Sze, *Physics of Semiconductor Devices* (Wiley, New York, 1984), 2nd ed.
5. J.B. Gunn, *IEEE Transactions on Electron Devices*, **ED-23**, 705 (1976)
6. R.W. Smith, *Phys. Rev. Lett.* **9**, 87 (1962)
7. G. Gruner and A. Zettl, *Phys. Rep.* **119**, 117 (1985)
8. B. Fisher, J. Genossar, K.B. Chashka, L. Patlagan and G.M. Reisner *Appl. Phys. Lett.* **88**, 152103 (2006); B. Fisher, J. Genossar, L. Patlagan and G.M. Reisner *J. Mag. Magn. Mat.* **322**, 1239 (2010), and references therein
9. B. Fisher, J. Genossar, L. Patlagan and G.M. Reisner, *J. Appl. Phys.* **111**, 023712 (2012)
10. B. Fisher, J. Genossar, A. Knizhnik, I. Patlagan and G.M. Reisner *J. Appl. Phys.* **103**, 023707 (2008)
11. B. Fisher, J. Genossar, L. Patlagan and G.M. Reisner, *J. Appl. Phys.* **109**, 084111 (2011)
12. F. Kohlrusch, *Ann. Phys. Lpz.* **1**, 132 (1900); H. Diesselhorst, *Ann. Phys. Lpz.* **1**, 312 (1900).
13. for a review see D.M. Kroll, *Phys. Rev. B* **9**, 1669 (1974)
14. S. Mercone, R. Fresard, V. Caignaert, C. Martin, D. Saurel, C. Simon, G. Andre, P. Monod and F. Fauth, *J. Appl. Phys.* **98**, 23911 (2005)
15. L.J. Zeng, H.X. Yang, Y. Zhang, H.F. Tian, C. Ma, Y.B. Qin, Y.G. Zhao, and J.Q. Li, *EPL* **84**, 57011 (2008); C.-H. Li, X.-Q. Zhang, Z.-H. Cheng, and Y. Sun, *Appl. Phys. Lett.* **93**, 152103 (2008); S. Cao, J. Li, H.F. Tian, Y.B. Qin, L.J. Zeng, H.X. Yang, and J.Q. Li, *Appl. Phys. Lett.*, **98**, 102102 (2011)
16. F.M. Vitucci, A. Nucara, C. Mirri, D. Nicoletti, M. Ortolani., U. Schade and P. Calvani, *Phys. Rev. B.* **84**, 153105 (2011)
17. J.S. Wen, G.Y. Xu, G.D. Gu, and S.M. Shapiro, *Phys. Rev. B* **81**, 144121 (2010).